Applied Thermal Engineering 29 (2009) 2508–2517

Contents lists available at ScienceDirect

Applied Thermal Engineering

journal homepage: www.elsevier.com/locate/apthermeng

CFD simulation of upward subcooled boiling flow of refrigerant-113 using the two-fluid model

Erfeng Chen, Yanzhong Li *, Xianghua Cheng

School of Energy and Power Engineering, Xi'an Jiaotong University, Xi'an 710049, China

ARTICLE INFO

Article history:
Received 9 August 2008
Accepted 23 December 2008
Available online 31 December 2008

Keywords:
Two-fluid model
Subcooled boiling flow
Temperature dependent properties
Saturation temperature variation
Refrigerant-113

ABSTRACT

In this paper, a modified two-fluid model considering temperature dependent properties and saturation temperature variation was adapted to accurately simulate the process of subcooled boiling flow. The calculations were performed by a CFD code CFX-10 with an extended user defined FORTRAN. The refrigerant-113 boiling flow experiments in a vertical concentric annulus from reference were used to validate the modified two-fluid model of subcooled boiling flow. Compared with the previous published predicted results, the results in the present model show better and reasonable approximation with the experimental data, including the local distribution of void fraction, liquid temperature, axial liquid and vapor velocity. Results show that with increasing the wall heat flux, the bubble boundary layer will become thicker, the liquid temperature gradient at the near-wall region will be smoother and the profiles of axial liquid velocity will gradually depart from those of single-phase flow. Decreasing the inlet liquid subcooling or the mass flux will obtain the same results.

1. Introduction

Subcooled boiling flow occurs in many technical applications of process and engineering, for example, steam generators, nuclear reactors and refrigeration systems. Subcooled boiling flow denotes the process of evaporation of subcooled liquid flowing near a heated surface, where the bulk flow temperature is lower than the local saturation temperature. It is characterized by the presence of thermodynamic non-equilibrium between the liquid and vapor phases, which increases the complexity of the process and makes the analysis of the process very challenging.

With the rapid development of computer technology and computational fluid dynamics (CFD), multidimensional theoretical description and analysis of subcooled boiling flow have being performed. Among these, the most widely used and effective approach so far appears to be two-fluid model. Two-fluid model was formulated in terms of two sets of conservation equations governing the balance of mass, momentum and energy of each phase, which were coupled with interfacial mass, momentum and energy transfer, respectively. First multidimensional two-fluid model of subcooled boiling flow was formulated and implemented by Kurul and Podowski [1]. Up to now, model improvements have being suggested and performed by other authors [2–8], and better numerical results have been accomplished against the published experimental data. Model improvements are usually concentrated on two-phase wall function, wall heat flux partition, bubble departure diameter, vapor bubble diameter etc., whereas few investigations have been done on the temperature dependent properties of fluid in subcooled boiling flow and saturation temperature variation along the heated channel. In Ref. [5], Koncar and Kljenak studied the saturation temperature variation in modelling the subcooled boiling flow of water at low pressure; however, no further analysis of the influence on the local characteristics of the subcooled boiling flow was performed.

In fact, for the refrigerants at low pressure the variations of liquid properties with subcooling and saturation temperature along the heated channel are relatively obvious. Taking refrigerant-113 for example, when liquid subcooling varies from 0 to 40 K, density, thermal conductivity, viscosity and specific heat at constant pressure increase by 6.7%, 13.5%, 57.1%, −4.7%, respectively. Moreover, the saturation temperature of refrigerant-113 at low pressure varies evidently along the heated channel (for about 5 K in a 3 m long vertical channel), which is closely correlative with the predictions of local flow characteristics in subcooled boiling flow. Therefore, temperature dependent properties and saturation temperature variation along the heated channel should be given extra considerations in order to accurately simulate the process of subcooled boiling flow.

In the present work, the general-purpose computational fluid dynamics code CFX-10 was used as a framework for solving the generic two-fluid model with additional relevant closure relations, and user defined CEL (CFX Expression Language) functions were

* Corresponding author. Tel.: +86 29 82668738; fax: +86 29 82668725.
E-mail addresses: cryo_efchen@yahoo.com.cn (E. Chen), yzli-epe@mail.xjtu.edu.cn (Y. Li).

1359-4311/$ - see front matter © 2008 Elsevier Ltd. All rights reserved.
doi:10.1016/j.applthermaleng.2008.12.022

acted as an important tool to implement the interfacial transfer models and the definition of temperature dependent properties. Moreover, the Arizona State University (ASU) boiling flow experiments [9,10] were used to validate the subcooled boiling model. Refrigerant-113 was taken as the working fluid both in experiments and simulations. Since refrigerants at low pressure posses the analogical properties with water at high pressure, it is assumed that those models used for predicting subcooled boiling flow of high pressure water can be similarly applied to the refrigerant-113 at low pressure. And on top of these, a modified two-fluid model considering temperature dependent properties and saturation temperature variation was adapted to accurately simulate the process of subcooled boiling flow. Further, by comparing with the experimental data and the previous predicted data calculated by Koncar and Krepper [8], the numerical results of local flow characteristics at the measurement plane were analyzed and discussed, including the local distribution of void fraction, liquid temperature, axial liquid and vapor velocity.

2. Two-fluid model of subcooled boiling flow

Two-fluid model of subcooled boiling flow is formulated in terms of two sets of conservation equations governing the balance of mass, momentum and energy of each phase. The macroscopic fields of one phase are not independent of the other phase, and the interaction terms which couple the inter-phase transfer of mass, momentum and energy across the interfaces appear in governing equations. The liquid phase is dominant and is described as continuous while the vapor bubbles are described as dispersed phase.

2.1. Wall boiling model

According to the mechanical model on subcooled boiling flow of Kurul and Podowski [1], the wall heat flux q_w is split into three different components: the single-phase convection heat flux $q_{1\phi}$, the quenching heat flux q_Q and the wall evaporation heat flux q_e, as shown in Fig. 1.

$$\begin{aligned} q_w &= q_{1\phi} + q_Q + q_e \\ &= S_t \rho_l c_{pl} A_{1\phi} u_l (T_w - T_l) + 2f(\tau_Q \lambda_l \rho_l c_{pl}/\pi)^{0.5} A_{bub}(T_w - T_l) \\ &\quad + N_a f \pi d_{bw}^3 \rho_g H_{lg}/6 \end{aligned} \tag{1}$$

where S_t is the local Stanton number, f is the bubble nucleation frequency, T_w is the wall temperature, T_l and u_l are the local liquid temperature and the velocity in the near-wall computational cell, respectively. The quenching period τ_Q between the departure of a bubble and the beginning of the growth of a subsequent one is defined as $\tau_Q = 0.8/f$. A_{bub} is the area fraction influenced by the nucleating bubbles and is usually formulated as $A_{bub} = \min[1, \pi N_a d_{bw}^2]$, where N_a is active nucleation sites density and d_{bw} is the bubble departure diameter. Whereas the remaining fraction $A_{1\phi} = 1 - A_{bub}$ is influenced only by the single-phase convection.

Lemmert and Chawla correlation and Cole correlation [7] were adopted to compute active nucleation sites density N_a and the bubble nucleation frequency f, respectively.

$$N_a = (185(T_w - T_l))^{1.805} \tag{2}$$

$$f = \sqrt{4g(\rho_l - \rho_g)/(3d_{bw}\rho_l)} \tag{3}$$

For the bubble departure diameter, a Tolubinsky and Kostanchuk correlation [7] was applied:

$$d_{bw} = \min(0.6[\text{mm}] \exp(-\Delta T_{sub}/45), 1.4[\text{mm}]) \tag{4}$$

2.2. Thermal phase change model

In subcooled boiling flow, the inter-phase heat and mass transfer between the two phases are described by the bubble evaporation on the heated wall (Section 2.1) and the bubble condensation in bulk flow. After departure from the heated wall, the vapor bubbles are supposed to be surrounded by subcooled liquid and become condensed. The process of phase change induced by inter-phase heat transfer in subcooled boiling flow can be simulated by thermal phase change model.

The rate of inter-phase heat transfer Q_{lg} across the phase boundary per unit time per unit volume is:

$$Q_{lg} = h_{lg} A_{lg} (T_g - T_l) \tag{5}$$

where, A_{lg} denotes the interfacial area density, which can be expressed as $A_{lg} = 6r_g/d_b$, and h_{lg} is the inter-phase heat transfer coefficient, defined as $h_{lg} = Nu_b \lambda_l / d_b$. For a particle in a moving incompressible Newtonian fluid, the bubble Nusselt number Nu_b can be calculated from the Ranz-Marshall correlation [7]:

$$Nu_b = 2 + 0.6 \mathrm{Re}_b^{0.5} \mathrm{Pr}_l^{1/3} \tag{6}$$

In Eq. (6), Re_b is the bubble Reynolds and Pr_l is the surrounding liquid Prandtl Number.

Correspondingly, the interfacial condensation rate Γ_{cond} across the phase boundary is deduced as:

$$\Gamma_{cond} = h_{lg} A_{lg} (T_g - T_l)/H_{lg} \tag{7}$$

2.3. Inter-phase momentum transfer

In the CFX-10 code, the inter-phase momentum transfer in subcooled boiling flow is usually modeled with the following interfacial forces [11]: drag force $\vec{F}_D$ and non-drag force such as lift force $\vec{F}_L$, turbulent dispersion force $\vec{F}_{TD}$ and wall lubrication force $\vec{F}_W$.

The drag force $\vec{F}_D$ is aroused by interfacial friction force and pressure difference acted on the vapor bubbles, which is computed by Ishii-Zuber correlation in the present work:

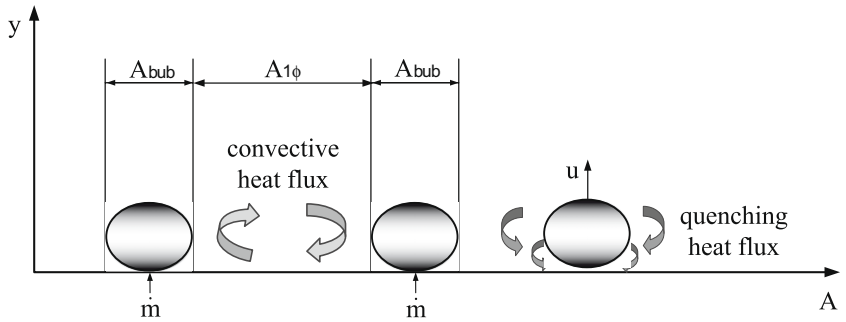

Fig. 1. Heat flux partition of the wall boiling model.

$$\vec{F}_D = \frac{3C_D}{4d_b} r_g \rho_l |U_g - U_l|(\vec{U}_g - \vec{U}_l) \tag{8}$$

where C_D represents the drag coefficient, and d_b denotes the bubble diameter.

The lift force $\vec{F}_L$ due to asymmetric wake and deformed asymmetric particle shape can be modeled as:

$$\vec{F}_L = C_L r_g \rho_l (\vec{U}_g - \vec{U}_l) \times \omega_g \tag{9}$$

The turbulent dispersion force $\vec{F}_{TD}$, based on the Favre average of the inter-phase drag force, is implemented in CFX-10 as follows:

$$\vec{F}_{TD} = C_{TD} \frac{3C_D \mu_l^{eff}}{4d_b \sigma_t} \left(\frac{\nabla r_g}{r_g} - \frac{\nabla r_l}{r_l} \right) \tag{10}$$

Here, σ_t is the turbulent Schmidt number of liquid phase with the value 0.9, C_{TD} denotes the turbulent dispersion coefficient which has a default value of 1.0.

The wall lubrication force $\vec{F}_W$ acts in lateral direction away from the wall and tends to push the vapor bubble away the heated wall. Herein the model of Antal et al. [12] is used for computing the wall lubrication force:

$$\vec{F}_W = -r_\beta \rho_\alpha \frac{(\vec{U}_g - \vec{U}_l)^2}{d_b} \max\left(C_1 + C_2 \frac{d_b}{y_w}, 0 \right) \vec{n} \tag{11}$$

In Eq. (11), y_w denotes the distance to the nearest wall, $\vec{n}$ is the unit normal pointing away from the wall, the coefficients C_1 and C_2 are −0.01 and 0.05, respectively.

3. Experimental facility and sensitivity analysis

The Arizona State University (ASU) boiling flow experiments [9,10] in a vertical concentric annulus were used to validate the modified two-fluid model of subcooled boiling flow. Refrigerant-113 was taken as the working fluid both in experiments and simulations.

3.1. Experimental facility

The subcooled boiling flow experiments of ASU [9,10] were carried out in a vertical annulus with a heated inner tube. The length of the heated part of the annulus is 2.75 m, while the inlet part of the test section (0.91 m) is not heated. The inner tube is made of the 304 stainless steel (I.D. = 14.60 mm, O.D. = 15.78 mm). The outer tube consists of two Pyrex tubes (I.D. = 38.02 mm, O.D. = 42.02 mm), which are connected by a 0.521 m long measurement section of optical quality quartz. The measurement plane (M.P.) is located 0.499 m downstream of the measurement section entrance, the entrance in turn being 1.56 m downstream of the beginning of the heated tube. The local measurements over the annulus cross-section were performed only at the measurement plane. The void fraction was measured by fiber-optic probe, and the axial vapor velocity was measured by two-component LDV and fiber-optic probe. Also, the axial liquid velocity and the liquid temperature were measured by two-component LDV and cold-wire, respectively. In the present work, six experimental cases, presented in Table 1, were simulated.

3.2. Numerical method

The test section was modeled as a 45° sector of the annular channel which has 20, 6 and 100 uniform grid cells in radial, circumferential and axial direction, respectively. Herein the length of the simulated test section was 3.66 m with a 2.75 m long upper heated part.

The calculations were performed with the finite volume code CFX-10 with an extended CFX-Executable including the FORTRAN routines for wall boiling model and thermal phase change model. The steady-state computational model was used. For the liquid phase a no-slip and for the gaseous phase a free slip boundary condition was used. Constant heat flux boundary condition was adopted on the heated wall and pressure boundary condition was applied at the outlet. Uniform velocity and temperature profiles were set at the inlet of the annulus channel. Besides, the two sections connected with heated wall along the annular channel were defined as symmetry planes. A k-ε turbulence model is employed for the continuous phase while the dispersed vapor phase remains laminar. The Sato's eddy viscosity model [13] is adopted to compute the bubble-induced turbulence viscosity.

The experimental case 6 was selected as the reference calculation, since only the distribution of local bubble diameters in this case was presented by the authors [9]. Fig. 2(a) and (b) show the predicted distributions of the void fraction and the liquid temperature in the annular channel. In order to explicitly exhibit the variation of void fraction and liquid temperature along the heated channel, a series of slices at an interval of 0.5 m are created, which the first slice is located 1.0 m downstream of the channel entrance.

3.3. Influence of temperature dependent properties

The influence of temperature dependent properties on the local characteristics of the subcooled boiling flow has been rarely discussed in former researches. Actually, for the refrigerant-113 at low pressure the variations of liquid properties with subcooling are relatively obvious. Table 2 shows the physical properties data of liquid refrigerant-113 (at 0.269 MPa) at different liquid subcoolings. When liquid subcooling varies from 0 to 40 K, density, thermal conductivity, viscosity and specific heat at constant pressure increase by 6.7%, 13.5%, 57.1%, −4.7%, respectively. Therefore, temperature dependent properties should be given extra considerations in order to accurately simulate the process of subcooled boiling flow. Fig. 3(a) and (b) present the influence of temperature dependent properties on the predicted void fraction profile and liquid temperature profile at the measurement plane. The "Constant properties" denotes the saturated liquid properties adopted, while "Variable properties" means that the liquid properties vary with liquid subcooling. Results indicate that actual liquid properties will produce the slightly lower void fraction profile and make the liquid temperature profile more close to the experimental data at the measurement plane, which can be explained by the liquid density difference between the "Constant properties" and "Variable properties". Compared with the saturated liquid properties, actual subcooled liquid possesses higher density than the saturated liquid, which means a larger inlet mass flux. That is to say, more heat flux will be required as the sensible heat to increase the liquid temperature, and eventually the slightly fewer vapor bubbles are generated. Moreover, as more subcooled liquid enters into the heated channel, the lower liquid temperature profile will be obtained, which better fits the experimental data at the measurement plane. In the whole, temperature dependent properties have little influence on the predictions of local flow characteristics in subcooled boiling flow, except that it represents a more actual inlet mass flux and makes the liquid temperature profile closer to the experimental data.

3.4. Influence of saturation temperature

In the original CFX-4 code of water subcooled boiling flow at high pressure, the saturation temperature may be defined only as a constant value over the entire flow domain. However, it is doubtful that constant saturation temperature is adopted for refrigerant-

Table 1
Experimental conditions of ASU.

Exp. No.	Pressure at M.P. (MPa)	Mass velocity (kg/m^{2}s)	Inlet velocity (m/s)	Inlet liquid temperature (K)	Wall heat flux (kW/m^2)
1	0.269	568	0.374	315.85	95
2	0.269	568	0.374	315.85	116
3	0.269	784	0.516	315.85	95
4	0.269	784	0.516	315.85	116
5	0.269	784	0.522	323.35	95
6	0.269	784	0.522	323.35	116

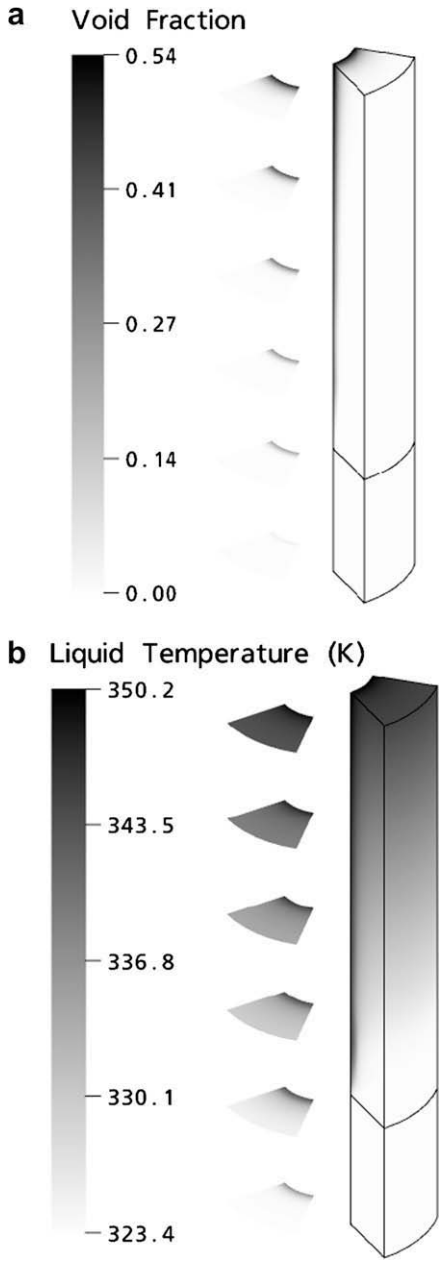

Fig. 2. Predicted distribution of void fraction and liquid temperature.

113 at low pressure condition, where the saturation temperature may vary evidently along the heated channel (for about 5 K in a 3 m long vertical channel). Three models of saturation temperature were simulated, including two constant saturation temperatures corresponding to the inlet pressure and the outlet pressure of heated channel, and a linear saturation temperature correlation between each other. Fig. 4(a) and (b) present the influence of the saturation temperatures on the predicted void fraction profile and liquid temperature profile at the measurement plane. When the saturation temperature drops, the evaporation heat flux will increase and the remainder heat flux used for heating liquid will decrease. Subsequently, more vapor bubbles will be generated and the liquid temperature at the near-wall region will be lower. On the other hand, as more vapor bubbles migrate to the bulk flow, the liquid temperature far from the heated wall will be higher. Compared with the experimental data, the linear saturation temperature correlation will be a reasonable choice for numerical simulation of refrigerant-113 subcooled boiling flow at low pressure.

3.5. Influence of vapor bubble diameter

In formulating a two-fluid model for predicting subcooled boiling flow, the local bubble diameter size is one of the important parameters required to estimate the interfacial transfer of mass, momentum and energy [2,14,15]. Vapor bubbles generated at the heated wall may slide along the wall, eventually depart and travel with the subcooled flow. Meanwhile the vapor bubbles may underlie the process of growth, departure, breakage and coalescence, which is very difficult to model the vapor bubble diameter distribution in the entire flow domain. As measured in the experiment case 6 of ASU, the probable vapor bubble diameters were between 0.7 mm and 1.3 mm at the measurement plane. Fig. 5(a) and (b) show the influence of the vapor bubble diameters (0.7, 1.3 mm and a mean diameter 1.0 mm) on the predicted void fraction profile and liquid temperature profile at the measurement plane. When the bubble diameter varies from 0.7 to 1.3 mm, the condensation rate, which is directly proportional to $1/d_b^2$, will decrease and makes the liquid temperature lower at the near-wall region. On the other hand, the large bubble diameter will produce the more powerful non-drag force, which makes less gas phase accumulated near the heated wall. Results indicate that the constant bubble diameter (1.0 mm) is an acceptable simplified method in the present work.

4. Results and discussions

Based on the above modified two-fluid model and the corresponding sensitivity analysis, six subcooled boiling flow experiments of ASU were simulated. Comparisons between the predicted local flow characteristics and experimental data in subcooled boiling flow are performed in the following sections at the measurement plane. Local flow characteristics include void fraction, liquid temperature, axial liquid velocity and vapor velocity. In order to show the application of the modified model, the predicted results of Koncar et al. [8] are compared and analyzed with the present work, too. Hereinafter, the prefix "Calc" means the predicted results using the modified model, while the prefix "Koncar" represents the calculated data in Ref. [8]. Incidentally, the partial vapor experimental data were substituted by the later subcooled boiling experimental data using a newly redesigned fiber-optic probe [10], for the results of only three experiments were presented in the short note.

Table 2
Physical properties data of liquid refrigerant-113 (at 0.269 MPa).

Subcooling (K)	Density (kg/m^3)	Therm. cond. (mW/m K)	Viscosity (μPa/s)	Cp (J/kg K)
0	1423	57.37	340.8	978.6
10	1450	59.26	379.3	966.0
20	1476	61.18	423.5	954.2
30	1501	63.13	474.9	943.2
40	1526	65.12	535.5	932.8

4.1. Void fraction

Fig. 6(a–c) presents the radial profile of the predicted and the experimental void fraction at the measurement plane. Compared the results calculated by Koncar et al., the predicted void fraction profiles using the modified model show better agreements with the experimental data. Especially, when the wall heat flux is 116 kW/m^2, the predictive error using the modified model is obviously small, while the two predicted results are approximate with the wall heat flux of 95 kW/m^2. Moreover, as the inlet liquid temperature increases, the predictive error is also smaller than that of the results calculated by Koncar et al. It means that the modified model of subcooled boiling flow shows a wide application when the liquid temperature in flow region is high. The local void fraction decreased from the heated wall to the subcooled liquid core, and the region extended by vapor bubbles can be defined as the bubble boundary layer. As shown in Fig. 6, when the wall heat flux

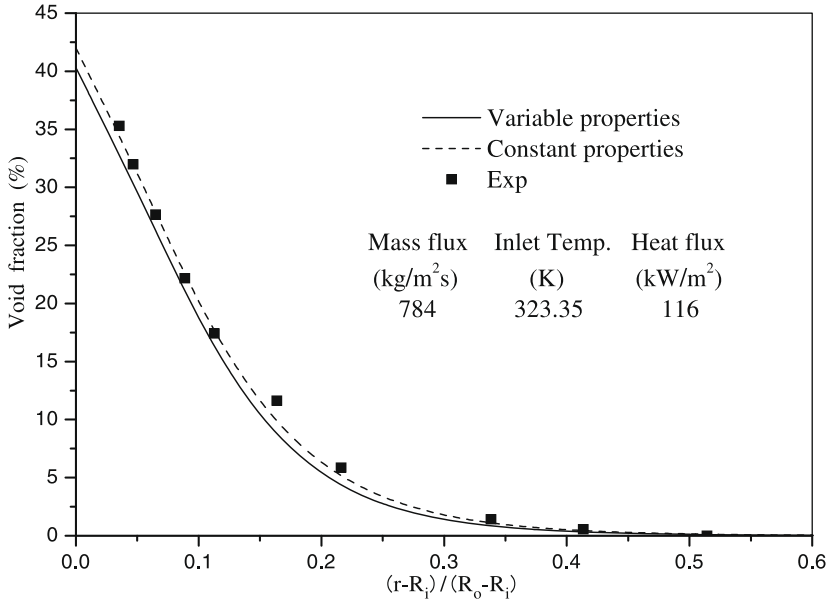

(a) Predicted void fraction profile at M.P.

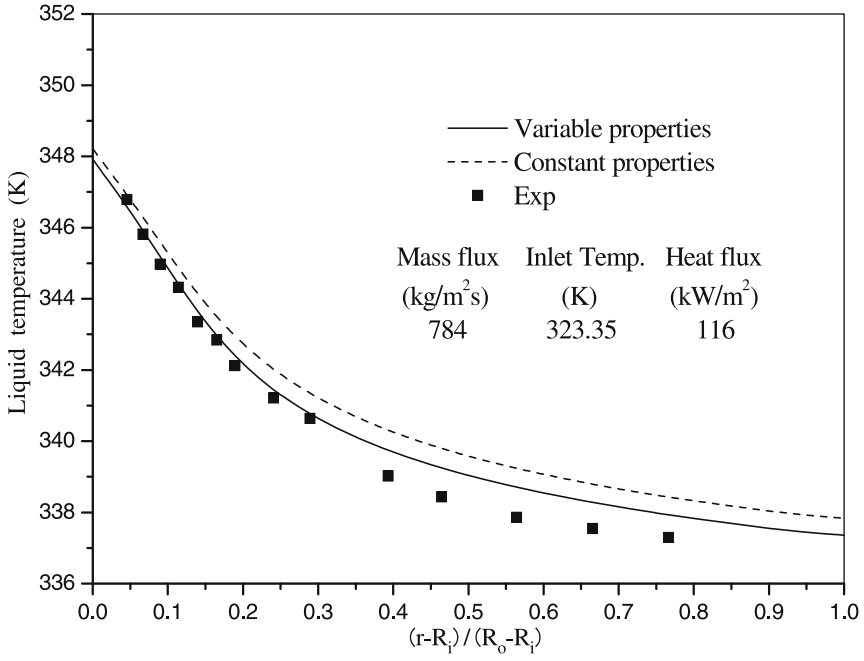

(b) Predicted liquid temperature profile at M.P.

Fig. 3. Influence of temperature dependent properties.

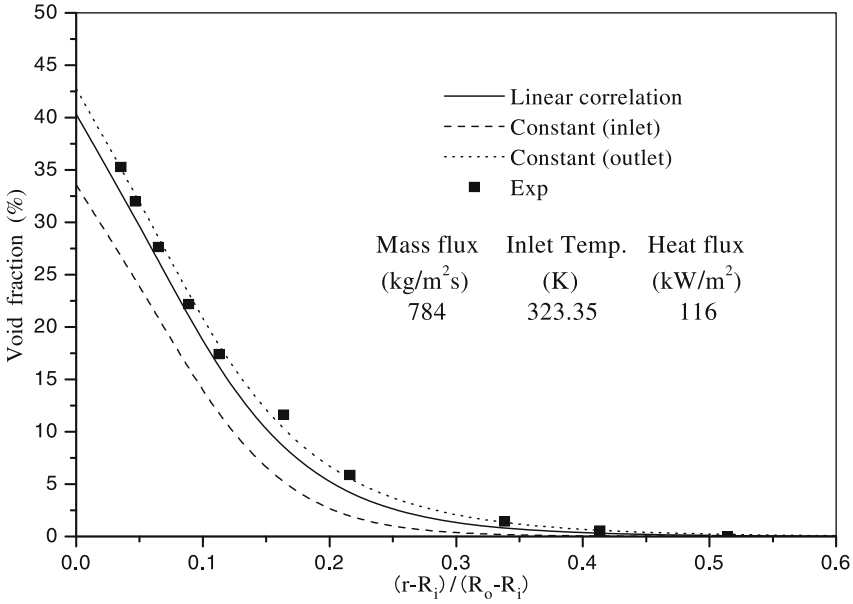

(a) Predicted void fraction profile at M.P.

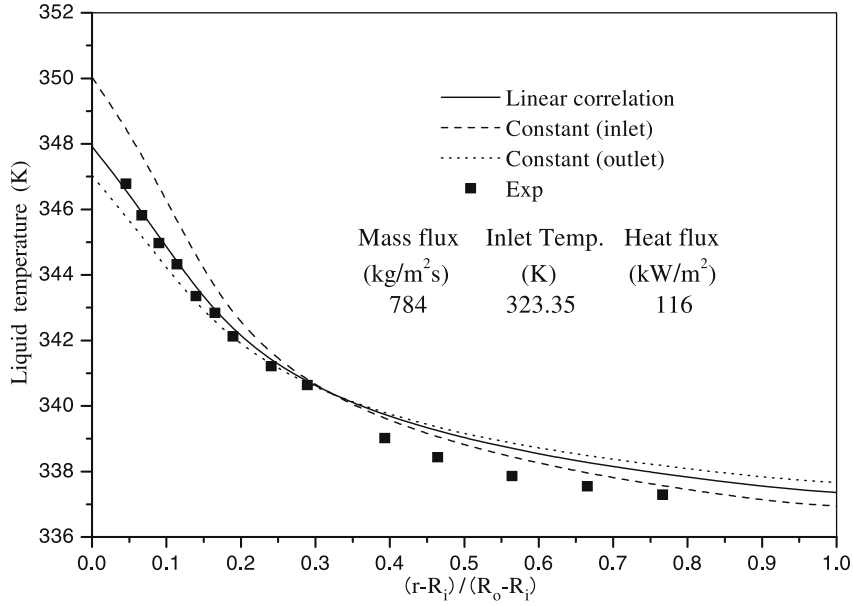

(b) Predicted liquid temperature profile at M.P.

Fig. 4. Influence of saturation temperature.

increases, the bubble boundary layer will become thicker, and the same results will be also obtained by decreasing the liquid subcooling or the mass flux.

4.2. Liquid temperature

Fig. 7(a–c) shows the radial profile of the predicted and the experimental liquid temperature at the measurement plane. In general, both the predicted results show the reasonable agreements with the experimental data. Compared with the results calculated by Koncar et al, the predicted results using the modified model are more close to the experimental data except at the near-wall region with low wall heat flux. As shown in Fig. 7, there is a high temperature gradient at the near-wall region, and the temperature gradient will decrease when approaching to the outer tube. Moreover, as the wall heat flux increases, the predicted and measured liquid temperature profiles become more smooth at the near-wall region, which can be interpreted by the increasing turbulent thermal diffusivity in flow region. The turbulent thermal diffusivity has the effect of smoothing the radial liquid temperature profile and can be enhanced by the radial motion of more vapor bubbles with high wall heat flux, which makes the liquid temperature profiles more smooth at the near-wall region. The same results will be also obtained by decreasing the liquid subcooling or the mass flux.

4.3. Axial liquid and vapor velocity

Figs. 8 and 9(a–c) show the radial profile of the predicted and the experimental axial liquid and vapor velocity at the measurement

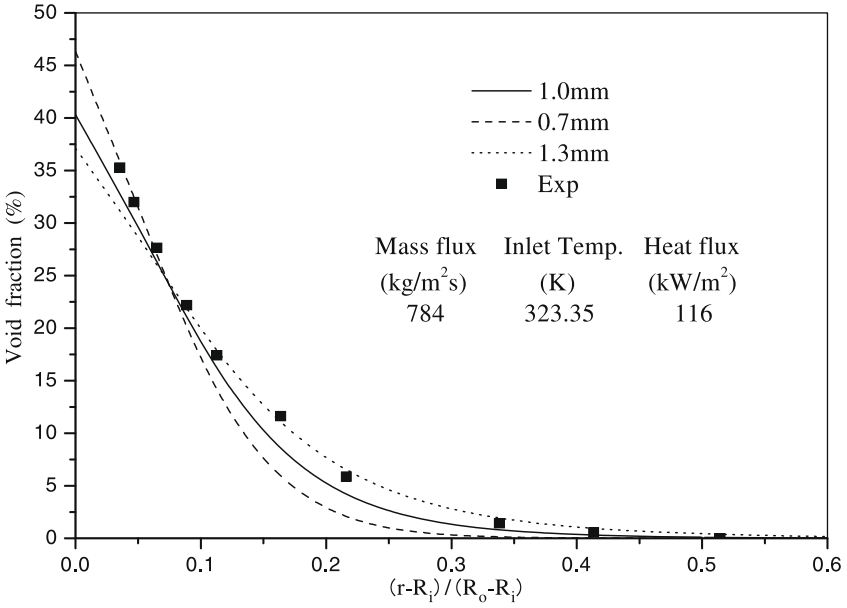

(a) Predicted void fraction profile at M.P.

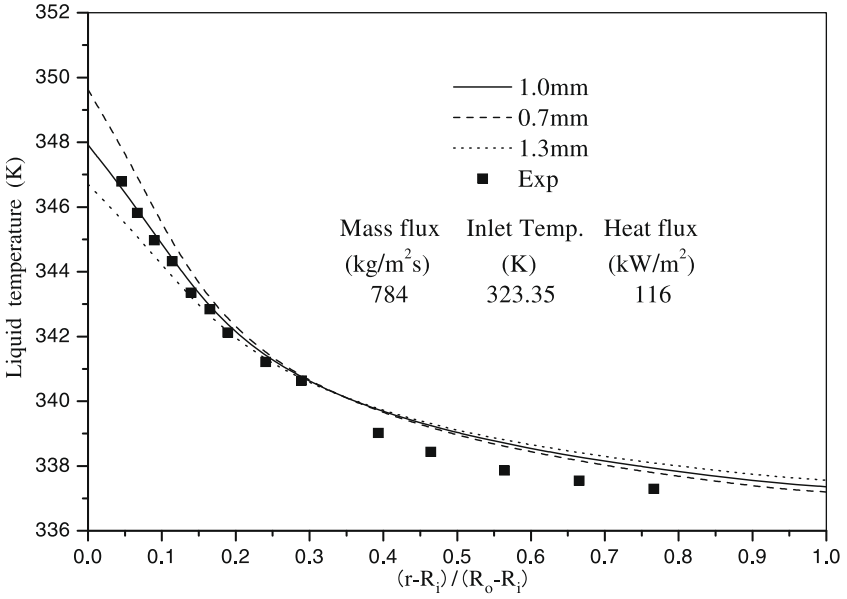

(b) Predicted liquid temperature profile at M.P.

Fig. 5. Influence of vapor bubble diameter.

plane, respectively. Obviously, the calculated axial vapor velocity profiles using the modified model show more advantages than the predicted results of Koncar et al, while the predictive error of axial liquid velocity is relative to the wall heat flux. When the wall heat flux is 116 kW/m^2, the predictive error with the experimental data using the modified model is higher than the results calculated by Koncar et al, whereas the predictive error is lower with the wall heat flux of 95 kW/m^2. Compared with the experimental data, large discrepancy occurs at the near-wall region for the axial liquid and vapor velocity profiles in the two predicted results, and the discrepancy will be enhanced with high wall heat flux. As the wall heat flux increases, high void fraction profile will be found in the bubble boundary layer at the measurement plane, which makes the vapor bubbles move faster than the bubbles in lower wall heat flux, and eventually develops the high predicted axial liquid velocity profile with the action of the inter-phase drag force. Similarly, when the wall heat flux is 116 kW/m^2, the large predictive error using the modified model can be also interpreted by the high void fraction distribution than the results predicted by Koncar et al. Especially, the axial liquid velocity in subcooled boiling flow has a peak value near the heated wall, while the axial liquid velocity has a maximum near the center of the channel in single-phase flow. Besides, as the mass flux increases, the profiles of axial liquid velocity gradually approach those of single-phase flow, which are described in Fig. 8(a) and (b). The same results of increasing inlet subcooling or decreasing the wall heat flux can be also seen in the Fig. 8. As shown in Fig. 9(a–c), the axial vapor velocity profiles show the similar trend with the axial liquid velocity profiles acted by the inter-phase drag force. However, the

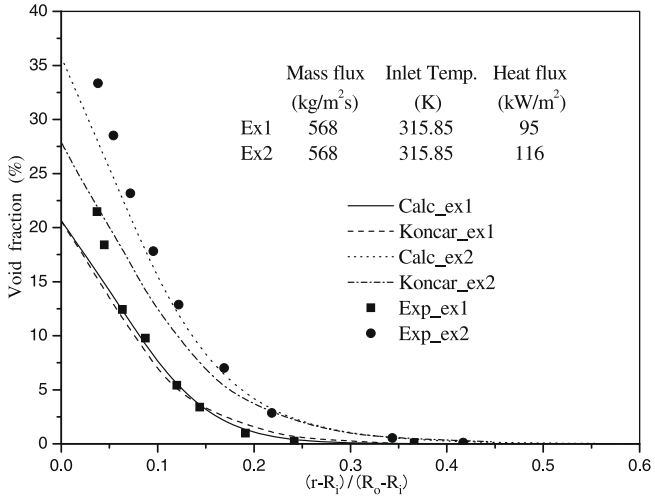

(a) Case 1 and case 2

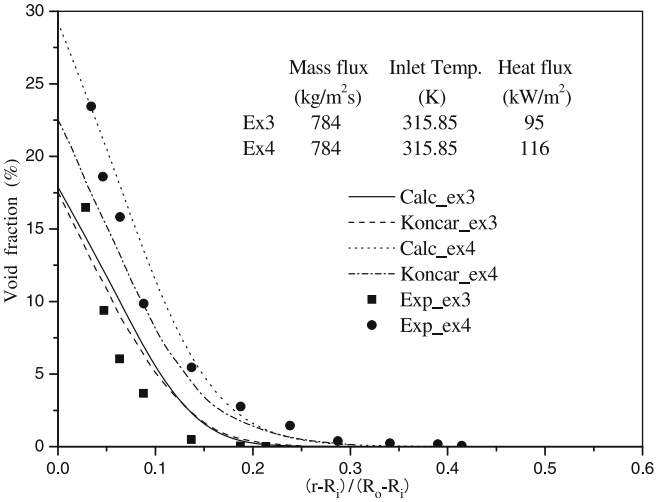

(b) Case 3 and case 4

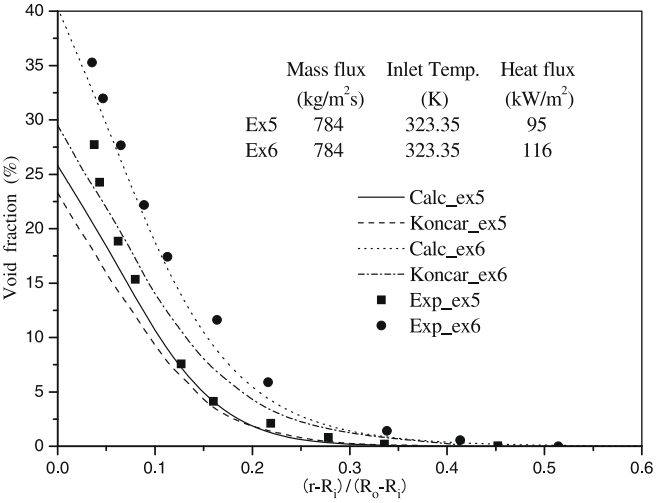

(c) Case 5 and case 6

Fig. 6. Void fraction: predicted and experimental profile at M.P.

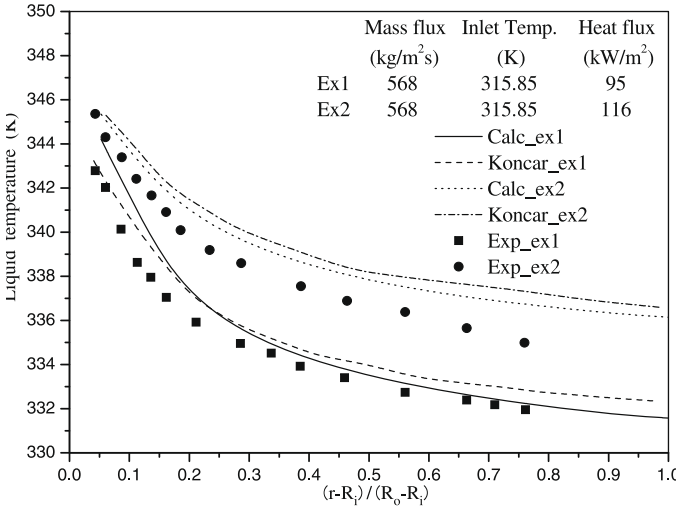

(a) Case 1 and case 2

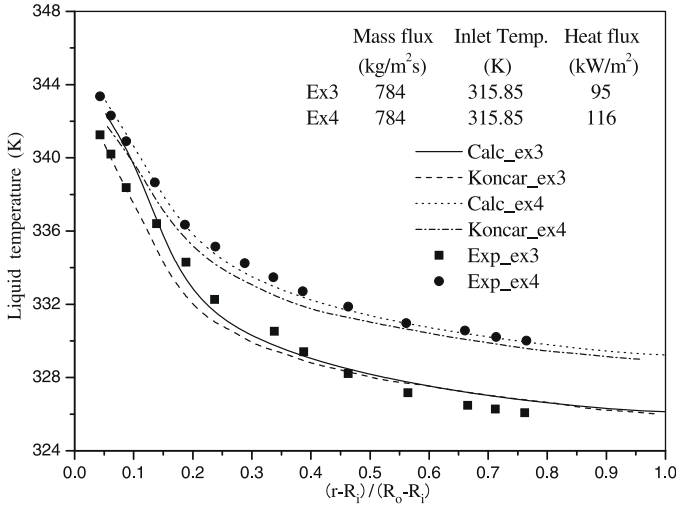

(b) Case 3 and case 4

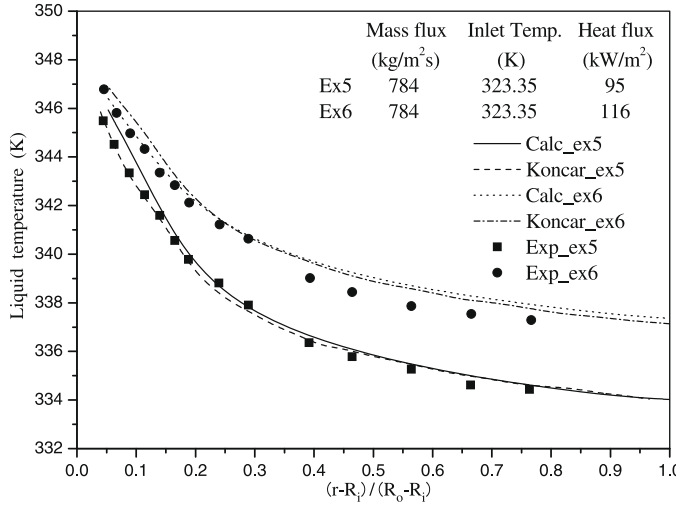

(c) Case 5 and case 6

Fig. 7. Liquid temperature: predicted and experimental profile at M.P.

quantitative difference of axial liquid and vapor velocity between the measurements and the predicted values is obvious. The discrepancy of the axial liquid and vapor velocity is mainly caused by the inter-phase momentum transfer, which underlines the need for improvement of dynamic models for momentum transfer.

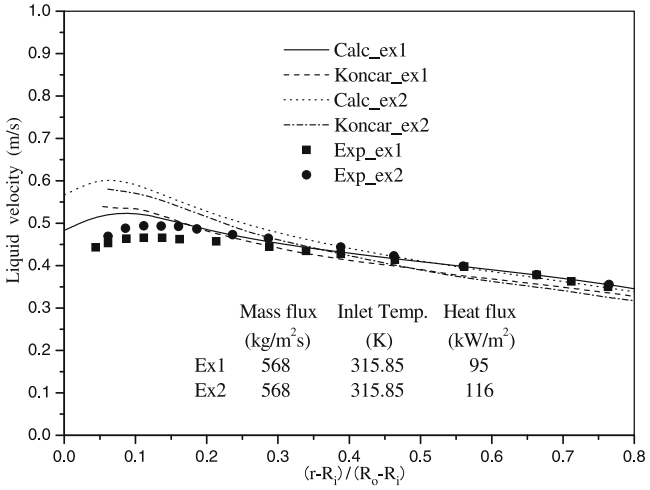

(a) Case 1 and case 2

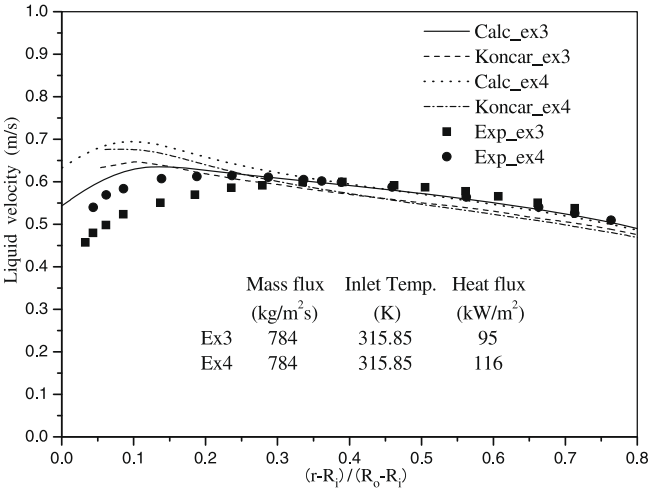

(b) Case 3 and case 4

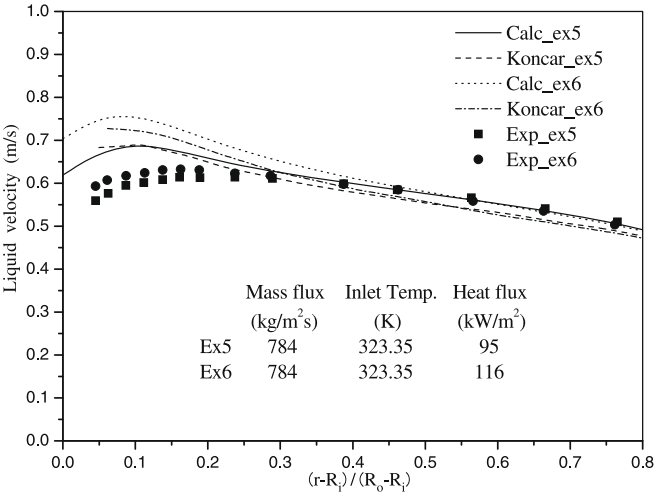

(c) Case 5 and case 6

Fig. 8. Liquid velocity: predicted and experimental profile at M.P.

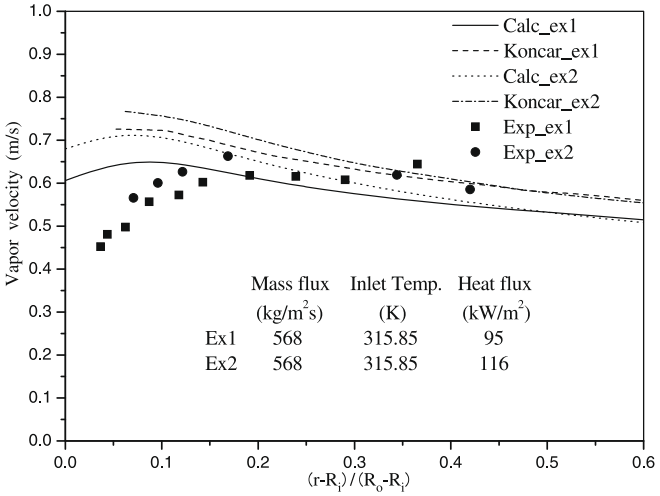

(a) Case 1 and case 2

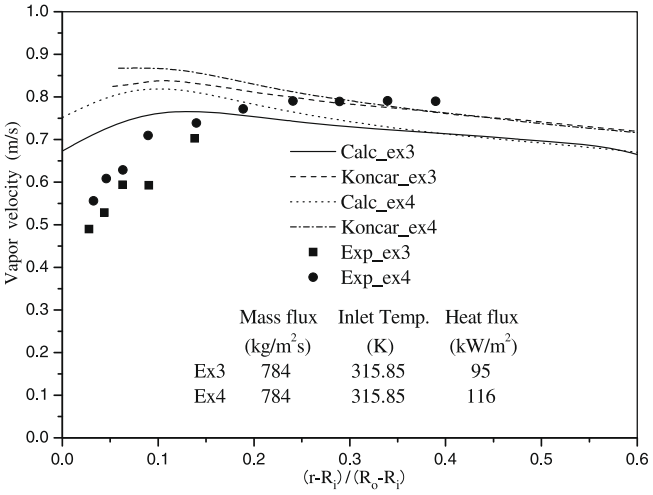

(b) Case 3 and case 4

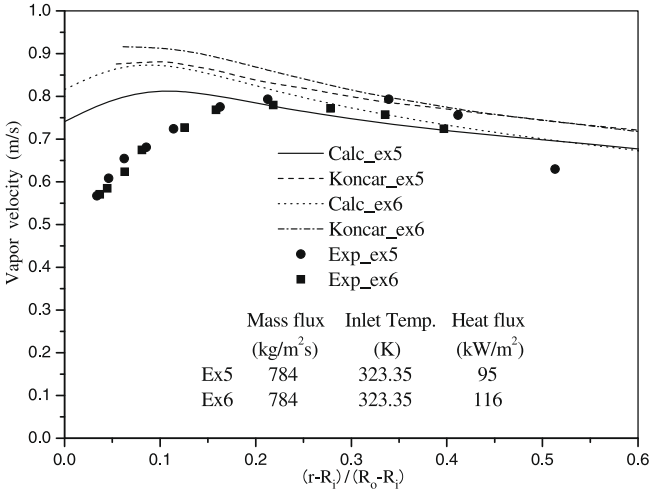

(c) Case 5 and case 6

Fig. 9. Vapor velocity: predicted and experimental profile at M.P.

5. Conclusions

The local flow characteristics of subcooled boiling flow of refrigerant-113 in a vertical concentric annulus have been numerically investigated with a modified two-fluid model, in which temperature dependent properties and saturation temperature variation along the flow direction was considered. The simulation results

were validated against the Arizona State University (ASU) boiling flow experiments. Results indicate temperature dependent properties have little influence on the predictions of local flow characteristics in subcooled boiling flow, except that it represents a more actual inlet mass flux and makes the liquid temperature profile more close to the experimental data. However, saturation temperature variation along the flow direction is an important influencing factor, which is closely correlative with the predictions of local flow characteristics in subcooled boiling flow. When the saturation temperature adopted is lower than the actual value, higher local void fraction profile and lower liquid temperature profile at the near-wall region will be predicted, and vice versa. Based on the modified two-fluid model considering temperature dependent properties and saturation temperature variation, numerical simulation of subcooled boiling flow of refrigerant-113 yielded better distributions of local flow characteristics.

Compared with the previous results predicted by Koncar et al., the calculated results using the modified model show better and reasonable approximation with the experimental data, including the local distribution of void fraction, liquid temperature, axial liquid and vapor velocity. Moreover, the modified model has a wide application with high wall heat flux, where the calculated results of Koncar et al. have large discrepancy except the profiles of axial liquid velocity. Results show that with increasing the wall heat flux, the bubble boundary layer will become thicker, the liquid temperature gradient at the near-wall region will be smoother and the profiles of axial liquid velocity will gradually depart from those of single-phase flow. Decreasing the liquid subcooling or the mass flux will obtain the same results.

Acknowledgements

This work was supported by National Science fund of China (50676074) and the Specialized Research Fund for the Doctoral Program of University by MOE China (20060698021). The author would like to thank the organizations above for their financial support.

References

[1] N. Kurul, M. Z. Podowski. On the modeling of multi-dimensional effects in boiling channels, in: 27th National Heat Transfer Conference, Minneapolis, 1991.
[2] J.Y. Tu, The influence of bubble size on void fraction distribution in subcooled boiling flow at low pressure, International Communication in Heat and Mass Transfer 26 (5) (1999) 607–616.
[3] N. Basu, G.R. Warrier, V.K. Dhir, Onset of nucleate boiling and active nucleation site density during subcooled flow boiling, Journal of heat transfer 124 (4) (2002) 717–728.
[4] J.Y. Tu, On numerical modeling of low pressure subcooled boiling flows, International Journal of Heat and Mass Transfer 45 (6) (2002) 1197–1209.
[5] B. Koncar, I. Kljenak, Modeling of local two-phase flow parameters in upward subcooled boiling flow at low pressure, International Journal of Heat and Mass Transfer 47 (6–7) (2004) 1499–1513.
[6] E. Krepper, D. Lucas, H.M. Prasser, On the modeling of bubbly flow in vertical pipes, Nuclear Engineering and Design 235 (5) (2005) 597–611.
[7] E. Krepper, B. Koncar, Y. Egorov, CFD modeling of subcooled boiling-concept, validation and application to fuel assembly design, Nuclear Engineering and Design 237 (7) (2007) 716–731.
[8] B. Koncar, E. Krepper, CFD simulation of convective flow boiling of refrigerant in a vertical annulus, Nuclear Engineering and Design 238 (3) (2008) 693–706.
[9] R.P. Roy, S. Kang, J.A. Zarate, A. Laporta, Turbulent subcooled boiling flow-experiments and simulations, ASME Journal of Heat Transfer 124 (73) (2002) 72–93.
[10] S. Kang, R.P. Roy, Vapor phase measurements in subcooled boiling flow, Journal of Heat Transfer 124 (6) (2002) 1207–1209.
[11] ANSYS-CFX Development Team. Solver Theory, Multiphase Flow Theory, CFX-5.7 Documentation, ANSYS, 2004.
[12] S.P. Antal, R.T. Lahey, J.E. Flaherty, Analysis of phase distribution in fully developed laminar bubbly two-phase flow, International Journal of Multiphase Flow 17 (5) (1991) 635–652.
[13] Y. Sato, M. Sadatomi, K. Sekoguchi, Momentum and heat transfer in two-phase bubble flow, International Journal of Multiphase Flow 7 (2) (1981) 167–177.
[14] D. Lucas, E. Krepper, H.M. Prasser, Prediction of radial gas profiles in vertical pipe flow on basis of the bubble size distribution, International Journal of Thermal Science 40 (3) (2001) 217–225.
[15] M.D. Bartel, M. Ishii, T. Masukawa, Y. Mi, R. Situ, Interfacial area measurements in subcooled flow boiling, Nuclear Engineering and Design 210 (1-3) (2001) 135–155.